

Cellular and Molecular Characterization of the Effects of the Zebrafish Embryo Genotyper Protocol

Alon M. Douek,* Emma I. Klein,* Jan Kaslin,
Peter D. Currie, and Avnika A. Ruparelia

Abstract

The Zebrafish Embryo Genotyper (ZEG) device provides a promising tool for genotyping live embryos. Although the gross morphology and survival of embryos after the use of ZEG are unaffected, the cellular and molecular effects of the ZEG protocol remain unknown. To address this, we have examined the integrity of specific tissues, and evaluated the expression of stress-responsive genes to determine the impact of the ZEG protocol. Our analyses reveal that although ZEG results in a low-level acute stress response, no long-lasting effects are evident, supporting its utilization for a variety of downstream assays.

Keywords: zebrafish genotyping, zebrafish embryo genotyper, ZEG

Introduction

THE RECENT DEVELOPMENT of the Zebrafish Embryo Genotyper (ZEG) device¹ has provided an automated method for genotyping of live zebrafish embryos, which has significant applications, including forward and reverse genetic screens, pharmacological assays, and multiomics experiments, whereby prior knowledge of the genotype of the animal is beneficial. The ZEG protocol involves dispensing zebrafish larvae onto a compartmentalized glass slide, which is subsequently subjected to vigorous microfluidic harmonic oscillations for ~8 min. This results in shedding of epidermal cells, from which genomic DNA is extracted for downstream genotyping assays. Although the ZEG protocol does not impact gross morphology and long-term survival of larvae,¹ the vigorous nature of the oscillation may affect cellular integrity and promote stress, thus potentially confounding downstream analyses. Therefore, using a combination of live confocal microscopy and quantitative real-time PCR (qPCR), we have examined the effects of ZEG treatment on cell morphology and the expression of several stress-response genes. Our results indicate that although low-level stress is induced immediately after the ZEG protocol, such stresses are not evident at a later stage, making it an appealing system for genotyping live embryos.

Methods

Fish husbandry and ZEG protocol

Fish maintenance was carried out as per the standard operating procedures approved by the Monash Animal Ethics Committee under breeding colony license ERM14481. Fish were anesthetized using 0.04% Tricaine methanesulfonate in

Australian Regenerative Medicine Institute, Monash University, Clayton, Australia.
*These authors are co-first authors.

embryo medium (5 mM NaCl, 0.17 mM KCl, 0.33 mM CaCl₂, 0.33 mM MgSO₄ in water). Fish strains used were the *Tübingen* wild-type strain, Tg(-3.0*mx1*:mTagBFP)^{mq10} (Ref.²), Tg(-3.5*ubb*:SEC-Hsa.ANXA5-mVenus,-0.6*cryaa*:mCherry)^{mq8} (Ref.³), double-transgenic Tg(*actc1b*:mCherry-CAAX, *actc1b*:lifeact-GFP)^{pc21.pc22} (Ref.⁴), and *dmd*^{pc2} (Ref.⁵). ZEG was performed on 2 days postfertilization (dpf) dechorionated embryos as per Lambert *et al.*¹ with the exception of the settings used which are 2.4 V, 0.051 A, and 0.12 W. Although *dmd*^{pc2} mutants were treated and imaged at 3 dpf, all other embryos were subjected to ZEG at 2 dpf, and subsequently imaged 1–3 h after ZEG treatment (0 days post-treatment [0 dpt]) and at 1 dpt.

Imaging

For analysis of autophagy, larvae were stained with LysoTracker Deep Red (L12492; Thermo Fisher Scientific) as per Ruparelia *et al.*⁶ For *in vivo* confocal microscopy, live embryos were mounted in 1% low melting temperature agarose (A9414; Sigma) and imaged using a Zeiss LSM 710 confocal microscope. Skeletal muscle birefringence was examined using an Abrio polarizing microscope as per previously established protocols.⁷ Images were blinded and randomized before analyses, and statistical significance was examined using a Student's *t*-test, two-sided Fisher's exact test or one-way analysis of variance.

Complementary DNA synthesis and qPCR

Total RNA was extracted from 8 to 10 larvae using TRI Reagent (93289; Sigma). Complementary DNA was synthesized from 500 ng total RNA per sample using Superscript III Reverse Transcriptase, and qPCR was performed using SYBR Green Master mix.

Results and Discussion

Since skeletal muscle, spinal cord, and motor neurons comprise most of the trunk, which is where the majority of damage is anticipated after the ZEG protocol, we specifically examined the structure of each of these tissues. Using cell-specific transgenic reporters, we reveal that ZEG treatment had no significant effect on the integrity of any of these cell types at either 0 or 1 dpt (Fig. 1A–D). Although our results highlight that ZEG does not impact cellular integrity in wild-type larvae, we hypothesized that it may compromise cell integrity in mutant strains that are more susceptible to damage. To test this, we subjected *dmd*^{pc2/pc2} mutants,⁵ which display compromised muscle integrity, to ZEG treatment and subsequently measured birefringence as a readout of skeletal muscle integrity. The treatment regime used was sufficient to extract amplifiable quantities of genomic DNA for PCR-based genotyping (Supplementary Fig. S1A). Although *dmd*^{pc2/pc2} mutants displayed a significant reduction in mean birefringence intensities compared with wild-type larvae (*dmd*^{+/+}), the mean birefringence of ZEG-treated *dmd*^{pc2/pc2} mutants was indistinguishable to that of untreated mutants (Fig. 1E, F), confirming that ZEG does not impact muscle integrity, even in a highly damage-susceptible context.

Having examined the impact of ZEG on cell integrity, we next examined its effects on inducing stress, specifically examining apoptosis and autophagy. Although we observed a moderate but nonsignificant increase in apoptotic signal in treated samples at 0 dpt (Fig. 1G, H), no difference was observed at 1 dpt. Autophagy, in contrast, was significantly elevated in ZEG-treated embryos at 0 dpt, although this phenotype resolved by 1 dpt (Fig. 1I, J). These data suggest that ZEG treatment may induce stress immediately after the protocol is performed, but these effects are transient. We further assessed the expression of a range of stress-/damage-associated genes. These include apoptosis-related genes *casp3a* and *casp3b*, oxidative stress-response genes: *sod1*, *sod2* and *cat*; the hypoxia-response gene *hif1ab*; immediate-early stress-response genes *jun*, *fosab*, *myca*, and *mycb*; and generalized stress-response genes *hsp70*, and *gstp1*. Our analyses reveal that although none of the stress-responsive genes are significantly upregulated after ZEG treatment, expression was found to be more variable in the treated groups (Fig. K, L; Supplementary Fig. S1B, C). This may be explained by uneven oscillation of the ZEG platform such that some wells vibrate more than others, resulting in varying levels of stress in each larva. This hypothesis is supported by the variable DNA amplification efficiency observed across different

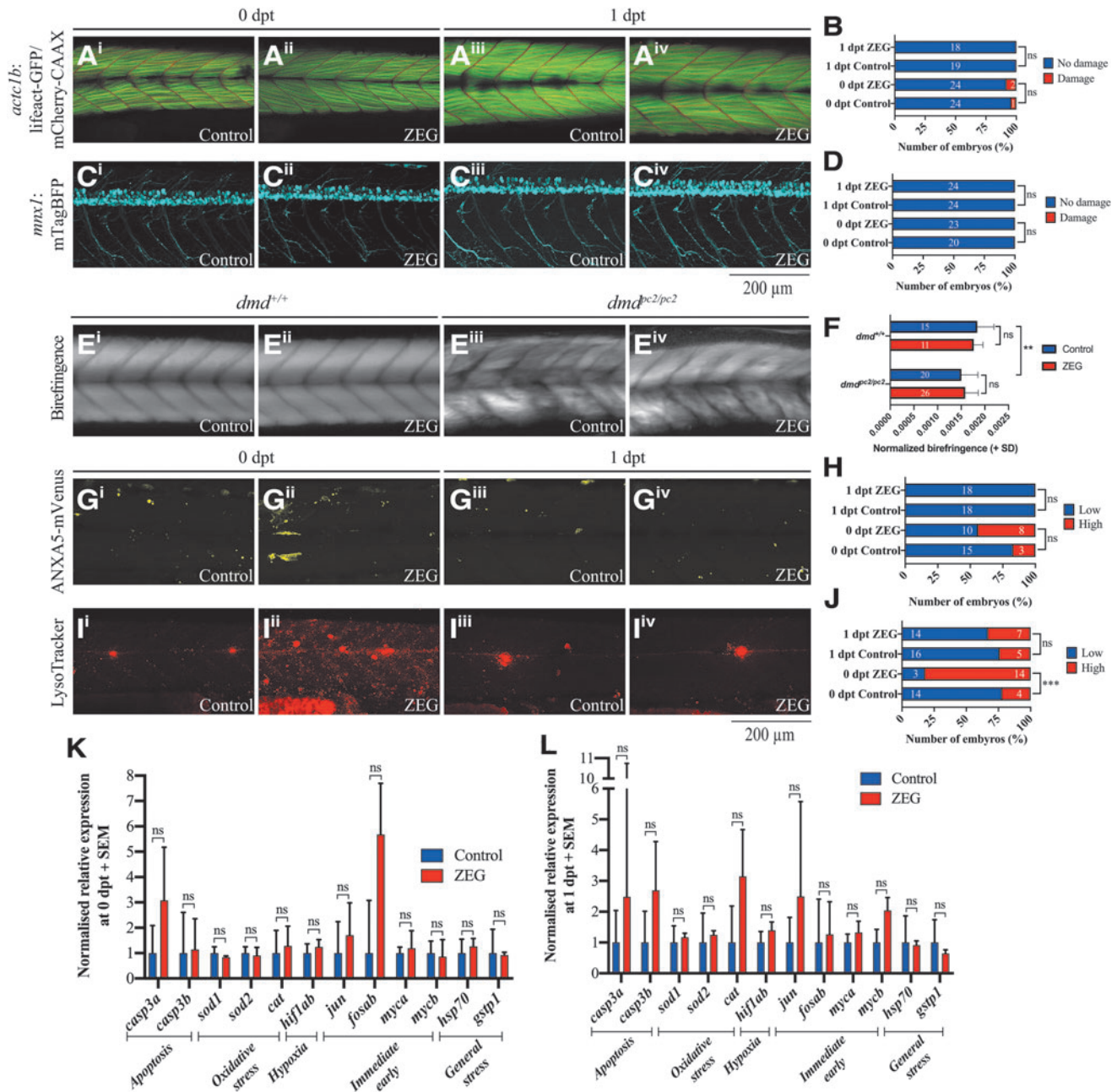


FIG. 1. Characterization of the cellular and molecular effects of ZEG treatment. Skeletal muscle integrity (A), assessed using the Tg(*actc1b*:mCherry-CAAX, *actc1b*:lifeact-GFP) strain, which labels muscle membranes (red) and fibers (green) was unaffected after ZEG treatment, as determined using a two-sided Fisher's exact test (B). The morphology of motor neurons (C) and spinal cord (C), identified using Tg(*mx1*:mTagBFP) line was also unaffected after ZEG treatment, as determined using a two-sided Fisher's exact test (D). *Dystrophin*-deficient larvae (*dmd*^{pc2/pc2}) display a significant reduction in skeletal muscle birefringence compared with wild-type siblings (*dmd*^{+/+}), which is not further exacerbated after ZEG treatment, determined using a one-way ANOVA with Sidak's multiple comparisons test. (E, F). Although abundance of apoptotic signal (ANXA5-mVenus) was not significantly changed in ZEG-treated larvae (G, H), LysoTracker staining, corresponding to autophagy levels, was significantly increased in ZEG-treated fish at 0 dpt but not at 1 dpt (I, J), as determined using a two-sided Fisher's exact test. Normalized relative expression of stress-response genes in control and ZEG-treated larvae at 0 dpt and 1 dpt (K, L). Error bars represent SEM for three replicate experiments with each experiment comprising pooled samples of 8–10 fish, and statistical significance determined using Student's *t*-test. ***p* < 0.05, ****p* < 0.001. ANOVA, analysis of variance; dpt, days post-treatment; ns, nonsignificant; SEM, standard error of the mean; ZEG, Zebrafish Embryo Genotype.

positions on the chip (Supplementary Fig. S1A). Therefore, there may be positional effects on the chip, which may increase variability in downstream experiments.

Collectively, our results indicate that vigorous oscillation from the ZEG protocol does not significantly impact global cell integrity, but may cause acute stress immediately after the regime. Based on these results, although ZEG treatment is unlikely to impact downstream experiments, we recommend waiting at least 24 h before performing these assays to ensure any residual effects of the ZEG regime have resolved, and advocate for the use of appropriate controls and randomization strategies to avoid bias from the use of ZEG.

Acknowledgment

We thank Monash Micro Imaging for assistance with the Abris polarizing microscope, and the staff of the Monash FishCore facility for zebrafish care and maintenance.

Disclosure Statement

No competing financial interests exist.

Funding Information

This study was supported by the National Health and Medical Research Council of Australia project grants to P.D.C.: APP1139253, APP1136567, and J.K.: GNT1145048, GNT1138870. The Australian Regenerative Medicine Institute is supported by grants from the State Government of Victoria and the Australian Government.

Supplementary Material

Supplementary Figure S1

References

1. Lambert CJ, Freshner BC, Chung A, Stevenson TJ, Bowles DM, Samuel R, *et al.* An automated system for rapid cellular extraction from live zebrafish embryos and larvae: development and application to genotyping. *PLoS One* 2018;13:e0193180.
2. Don EK, Formella I, Badrock AP, Hall TE, Morsch M, Hortle E, *et al.* A Tol2 gateway-compatible toolbox for the study of the nervous system and neurodegenerative disease. *Zebrafish* 2017;14:69–72.
3. Morsch M, Radford R, Lee A, Don EK, Badrock AP, Hall TE, *et al.* In vivo characterization of microglial engulfment of dying neurons in the zebrafish spinal cord. *Front Cell Neurosci* 2015;9:321.
4. Berger J, Tarakci H, Berger S, Li M, Hall TE, Arner A, *et al.* Loss of Tropomodulin4 in the zebrafish mutant *träge* causes cytoplasmic rod formation and muscle weakness reminiscent of nemaline myopathy. *Dis Models Mech* 2014;7:1407–1415.
5. Berger J, Berger S, Jacoby AS, Wilton SD, Currie PD. Evaluation of exon-skipping strategies for Duchenne muscular dystrophy utilizing dystrophin-deficient zebrafish. *J Cell Mol Med* 2011;15:2643–2651.
6. Ruparelia AA, Oorschot V, Vaz R, Ramm G, Bryson-Richardson RJ. Zebrafish models of BAG3 myofibrillar myopathy suggest a toxic gain of function leading to BAG3 insufficiency. *Acta Neuropathol* 2014;128:821–833.
7. Berger J, Sztal T, Currie PD. Quantification of birefringence readily measures the level of muscle damage in zebrafish. *Biochem Biophys Res Commun* 2012;423:785–788.

Address correspondence to:

Avnika A. Ruparelia, PhD
 Australian Regenerative Medicine Institute
 Monash University
 Clayton 3800
 Australia

E-mail: avnika.ruparelia@monash.edu